Nuclear matter within the continuous choice

M. Baldo, I. Bombaci, L. S. Ferreira,* G. Giansiracusa, and U. Lombardo
Instituto Nazionale di Fisica Nucleare, Sezione di Catania, Corso Italia 57, 95129 Catania, Italy
and Dipartimento di Fisica, Universitá di Catania, Corso Italia 57, 95129 Catania, Italy
(Received 27 November 1990)

The saturation curve of symmetric nuclear matter is calculated at the Brueckner-Hartree-Fock level of approximation within the continuous choice for the single-particle potential. The realistic local Argonne v_{14} potential is used and the results are compared with similar calculations presented in the literature. The binding energies per nucleon around saturation agree closely with previous results obtained with separable versions of the same potential as well as of the Paris potential.

I. INTRODUCTION

Nuclear matter properties have been extensively studied by many authors in the framework of the Brueckner-Bethe-Goldstone (BBG) theory where a hole-line expansion for the ground-state energy is generated.[1] In this expansion, the Goldstone or Hughenholtz diagrams are grouped according to the number of hole lines which they contain, and each group is summed up separately. The summation of the two-hole-line diagrams gives the usual Brueckner approximation, which requires the two-body scattering G matrix in nuclear matter to be calculated self-consistently with the single-particle energy spectrum. The summation of the three-hole diagrams can be performed by solving the Bethe-Faddeev equations,[2] which gives the three-nucleon scattering matrix in nuclear matter once the two-body G matrix has been determined. This hierarchy of equations can be continued to sum up sets of diagrams with a higher number of hole lines, but the numerical difficulties become prohibitive. So far, only the contribution of the four-hole-line diagrams has been estimated.[3]

The rate of convergence of the hole expansion has been checked by Day[3] and Day and Wiringa,[4] within the standard (or gap) choice, where the single-particle potential is assumed to be equal to the self-consistent Brueckner-Hartree-Fock (BHF) potential only for states with momenta below the Fermi momentum (and zero otherwise). Although the single-particle potential is introduced only as an auxiliary quantity, at least for the calculation of the total binding energy, its choice affects the convergence rate of the expansion. It has been argued[5] that, by adopting the self-consistent BHF potential for all momenta as the auxiliary potential (the continuous choice), one could include higher-order correlations within the two-hole-line approximation. This conjecture has been confirmed by some recent results[6] obtained for a separable version of the Paris[7] and Argonne[8] v_{14} potentials. In particular, it has been shown[6] that the saturation curve calculated in the latter approximation largely overlaps with the one including the three-hole-line contribution in the gap choice.

Unfortunately, there is no agreement in the literature among the different calculations performed within the continuous choice. The results presented in Refs. 9 and 10 for the Paris potential are in disagreement between each other and exhibit larger deviations from the calculations mentioned above. These discrepancies have been pointed out in Ref. 11 and require a careful reexamination to check the validity of the conclusions reached in Ref. 6. Calculations made with the Paris and Argonne v_{14} potentials agree quite closely within the gap choice when the two potentials are considered in both their exact[4] or separable[8] forms. Therefore, we expect that, in the continuous choice also, the two potentials will be essentially equivalent. Indeed, their separable forms[8,12] show an almost complete agreement. In this paper we present the results for the nuclear matter saturation curve, calculated within the continuous choice, for the Argonne v_{14} potential, without resorting to a separable version of the potential. In Sec. II the method of solution of the Brueckner equation is explained and checks on the method are also reported. The results are presented in Sec. III, where the conclusions are drawn as well.

II. METHOD OF SOLUTION

The calculations have been performed in the momentum representation, where the Brueckner equation for the two-body G matrix reads

$$\langle k_1'k_2'|G(\omega)|k_1k_2\rangle=\langle k_1'k_2'|v|k_1k_2\rangle+\sum_{k_3k_4}\langle k_1'k_2'|v|k_3k_4\rangle\frac{Q(k_3,k_4)}{\omega-E(k_3,k_4)}\langle k_3k_4|G(\omega)|k_1k_2\rangle\ , \tag{1}$$

where v is the bare potential, in our case, the Argonne v_{14}, Q is the Pauli operator which requires the nucleon momenta to be outside the Fermi sea, E is the sum of the two single-particle energies inside nuclear matter given by

$E(k_1,k_2)=e(k_1)+e(k_2)$ with $e(k)=k^2/2m+U(k)$, U being the self-consistent single-particle potential, and m is the nucleon mass ($\hbar=1$). The ket $|k\rangle$ indicates plane-wave states, normalized to 1 in a box.

In order not to mix different channels, an angle averaging has to be performed on the Pauli operator and the energy denominator before expanding in partial waves. This introduces an approximation which is expected to be accurate.

Performing the partial-wave expansion of Eq. (1), the coupled equations for the reaction matrix $G^{\alpha}_{LL'}(q,q',P;\omega)$ become, in the continuous limit,

$$G^{\alpha}_{LL'}(q,q',P;\omega)=v^{\alpha}_{LL'}(q,q')+\sum_{L''}\int q''^2 dq'' v^{\alpha}_{LL''}(q,q'')\frac{Q(q'';P)}{\omega-E(q'',P)}G^{\alpha}_{L''L'}(q'',q',P;\omega)\ , \tag{2}$$

where Q is the angle-averaged Pauli operator whose explicit expression is

$$Q(q,P)=\begin{cases}0, & q\le(k_F^2-\frac{1}{4}P^2)^{1/2}\ ,\\ 1, & q\ge k_F+\frac{1}{2}P\ ,\\ (q^2+\frac{1}{4}P^2-k_F^2)/qP & \text{otherwise}\ ,\end{cases}$$

with q and P the relative and total momentum of the two nucleons, respectively, and k_F the Fermi momentum. Finally, $\alpha\equiv\{JST\}$ specifies the set of conserved quantum numbers, the total angular momentum, spin and isospin for a given channel, while the quantities L,L',L'' are the orbital angular momenta.

The Argonne v_{14} potential has simple analytical expression in each channel, therefore, the Fourier transform is readily obtained and we have used the same grid in coordinate space as in Ref. 4.

The main difficulty in solving Eq. (2) within the continuous choice is the appearance of a singularity in the integrand whenever the energy ω is larger than twice the Fermi energy. These values of ω occur in the calculation of the self-consistent potential

$$U(k_1)=\sum_{k_2\le k_F}\langle k_1k_2|G(\omega)|k_1k_2\rangle_A \tag{3}$$

with $\omega=e(k_1)+e(k_2)$, whenever the momentum $k_1\ge k_F$. The subscript A indicates antisymmetrization. Special care has to be taken in numerically handling singular integral equations. We assume that, in the integral equation, the integral exists as a principal part integral. In the following, the method used in this work is briefly explained, together with the test calculations that have been done to control its precision. We assume that the two-particle energy $E(q'',P)$ appearing in the integral equation (2) is a monotonic function of the relative momentum q'', so that only first-order zeros can occur in the denominator. This is true if the single-particle potential is a monotonic function, at least in the range of momentum where it is non-negligible in comparison with the kinetic energy, and, anyhow, the assumption can be explicitly checked *a posteriori*. The momenta are discretized in a grid $\{q_i\}$ up to a cutoff momentum $q_{\max}$, which is taken to be 10 fm^{-1}. In each interval (q_i,q_{i+1}), the denominator in the integral is approximated by a straight line, while the numerator, including the unknown G matrix, is approximated by its arithmetic mean value. Then, in each interval, the integration can be done analytically, *irrespective* of the occurrence of the singularity in the interval, and the integral on the full interval is replaced by a discrete summation. For a grid of points large enough, the sum converges to the exact value of the integral, provided the G matrix is a smooth function of the momenta. The integral equation (2) is replaced by the set of linear equations

$$\sum_{j,L''}[\delta_{ij}\delta_{L,L''}+K^{\alpha}_{iL;jL''}(\omega)]G^{\alpha}_{L''L'}(q_j,q_k,P;\omega)=v^{\alpha}_{LL'}(q_i,q_k)\ , \tag{4}$$

where

$$\begin{aligned}&K^{\alpha}_{iL;jL''}(\omega)=v^{\alpha}_{LL''}(q_i,q_j)q_j^2Q(q_j,P)\theta_j(\omega)\ ,\\ &\theta_1=\tfrac{1}{2}R_1\ ,\quad \theta_N=\tfrac{1}{2}R_{N-1}\ ,\\ &\theta_i=\tfrac{1}{2}(R_i+R_{i-1})\ ,\quad i=2,\ldots,N-1\ ,\\ &R_i=(q_{i+1}-q_i)\ln\left|\frac{\omega-D_{i+1}}{\omega-D_i}\right|\Big/(D_{i+1}-D_i)\ ,\\ &D_i=E(q_i,P)\ ,\end{aligned} \tag{5}$$

with N the number of points in the momentum grid. More details on the derivation of Eq. (4) are given in the Appendix. For the purpose of the calculation we used as momentum grid $\{q_i\}=0.(0.1)5(0.25)10$ fm^{-1}.

To check the precision of the method of solution, we have calculated the scattering phase shifts in different channels for two free nucleons. For this purpose we have used the computer program to solve Eq. (2) for the G matrix and put the Pauli operator $Q(q,P)$ identically equal to 1 and the single-particle potential $U(k)$ equal to zero. The solution of Eq. (2) then provides the standing-wave K matrix for two-nucleon scattering, from which the phase shifts can be obtained. The phase shifts have also been obtained by solving the two-nucleon Schrödinger equation in coordinate space, following the method described in Ref. 13, where the Lippmann-Schwinger equation was solved in the interval $0<r<6.5$ fm, subdivided into eight subintervals of eight Gaussian points each. The comparison is made in Table I for the channels $^1S_0$ and $^3S_1$. The phase shifts agree with the ones reported in Ref. 14, at least within graphical accuracy. It has to be stressed that, for the $^3S_1$ channel, the free K matrix has a singu-

TABLE I. Phase shifts obtained with the method described in the text (k space), compared with ones obtained with the method of Ref. 13 (r space).

Channel	$^1S_0$		$^3S_1$	
k (fm^{-1})	k space	r space	k space	r space
0.5	0.901	0.896	1.494	1.477
0.8	0.672	0.656	1.059	1.053
1	0.517	0.500	0.845	0.834
1.2	0.365	0.350	0.656	0.645
1.6	0.079	0.071	0.333	0.328
2	−0.181	−0.182	0.063	0.067

larity at low energy, since the corresponding phase shift passes through $\pi/2$. Despite the fact that this method can present difficulties in this delicate case, the agreement can be considered quite satisfactory. It has to be noticed that this case never occurs in nuclear matter calculations. Obviously, the energy ω appearing in Eq. (4) cannot exactly coincide with one of the energy $q_i^2/2m$ of the grid. So, the G matrix has been calculated at the energies

$$\frac{1}{2m}\left[\frac{q_i+q_{i+1}}{2}\right]^2,$$

that is, in between two consecutive grid points, and finally interpolated linearly in the energy variable to get its value exactly on shell.

In order to test the method when no singularity is present in the integral equation, we performed a nuclear matter calculation in the gap choice scheme, for which comparison with results existing in the literature is possible. In Table II the contribution of each channel to the binding energy of symmetric nuclear matter, obtained from a self-consistent calculation at the Fermi momentum $k_F=1.4$ fm^{-1}, is reported in comparison with the work of Ref. 4. Notice that we have not included the $^3D_3$-$^3G_3$ channel in our calculation, which, however, gives quite a small contribution to the binding energy. The close agreement found indicates the accuracy of the method and also provides a test of the computer code.

TABLE II. Potential energy per particle in MeV for the Argonne v_{14} interaction in the gap choice, compared with the calculation of Ref. 4 at $k_F=1.4$ fm^{-1}.

Channel	Authors	Ref. 4
$^1S_0$	−17.18	−17.16
$^3S_1$	−17.51	−17.63
$^3P_0$	−4.12	−4.11
$^3P_1$	12.29	12.17
$^1P_1$	4.56	4.52
$^3P_2$	−7.72	−7.65
$^1D_2$	−3.21	−3.17
$^3D_2$	−4.67	−4.62
$^3D_1$	1.61	1.60
$l\geq 3$	0.59	0.79
Kinetic energy	24.38	24.38
Total binding	−10.87	−10.88

III. THE CONTINUOUS CHOICE: RESULTS AND CONCLUSIONS

In the continuous choice, the single-particle potential of Eq. (3) is calculated self-consistently, with an iterative procedure, up to a cutoff momentum, which we took at $k=4$ fm^{-1}. The total potential energy at the two-hole level is given by

$$B=\frac{1}{2}\sum_{k_1k_2\leq k_F}\langle k_1k_2|G(\omega)|k_1k_2\rangle_A\ , \tag{6}$$

where the single-particle momenta are inside the Fermi sea and the energy parameter $\omega=e(k_1)+e(k_2)$. For simplicity and for the sake of comparison, we followed the prescription of Ref. 10 and the G matrix has been calculated for an average total momentum $P=\sqrt{6/5}k_F$. To check this approximation we have also performed a calculation at the density corresponding to $k_F=1.75$ fm^{-1} using a grid, with 0.5 fm^{-1} step size, for the total momentum P and linearly interpolating the G matrix in P. We found that the binding energy changes only about 300 keV. Smaller changes are expected at lower densities.

The saturation curve of symmetric nuclear matter within the continuous choice for the Argonne v_{14} potential is shown in Fig. 1, in comparison with similar calculations made by the authors of Refs. 9 and 10 for the Paris potential. As previously stated, the observed differences cannot be ascribed to the use of a different po-

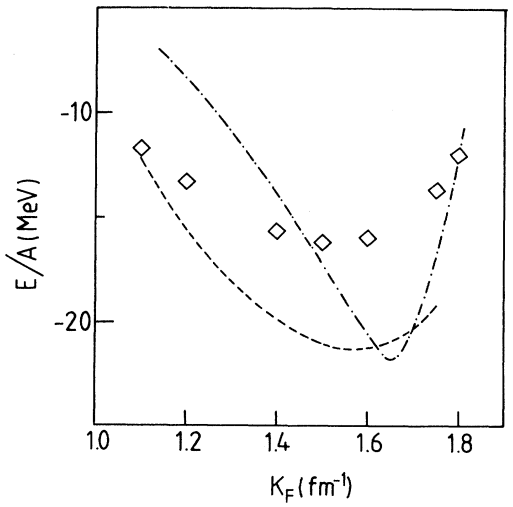

FIG. 1. Binding energy per nucleon as a function of Fermi momentum in the "continuous" choice. The calculation for the Argonne v_{14} potential, represented by the squares, is compared with the calculations with the Paris potential of Refs. 9 and 10, dash-dotted and dashed lines, respectively.

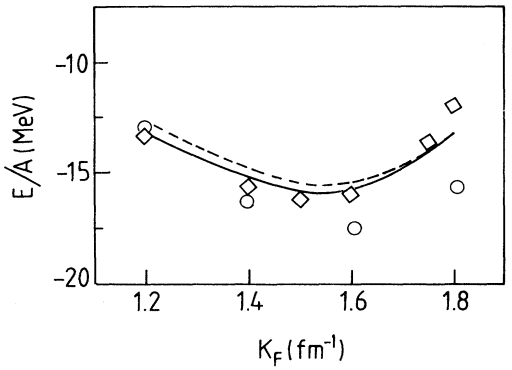

FIG. 2. Binding energy per nucleon as a function of Fermi momentum in the "continuous" choice for the separable representations of the Paris and Argonne potentials, full and dashed lines, respectively in comparison with the results, squares, for the local Argonne v_{14} potential. The circles indicate the results of Ref. 4, which include three- and four-hole estimates in the gap choice for the Argonne v_{14} potential.

tential. In fact, performing a continuous choice calculation with the separable version of the Paris potential and of the Argonne v_{14} potential, one gets results quite close to each other and to the one of the original local Argonne v_{14}, as shown in Fig. 2. For comparison, the results obtained with the three- and four-hole diagrams estimated in the gap choice and for the Argonne v_{14} potential are also reported in Fig. 2. One can notice that the continuous choice makes the BHF calculation approach the results of Ref. 4. In Table III the contribution of each channel to the potential energy of symmetric nuclear matter obtained for the Argonne v_{14} potential in the gap and continuous choice are compared for various values of the Fermi momenta. It is interesting to notice that the difference between the results in the gap and continuous choice is mainly observed in the $^3S_1$-$^3D_1$ channel.

In summary, we have presented the calculation of the saturation curve for the symmetric nuclear matter at the two-hole level of approximation within the continuous choice for the single-particle potential and for the realistic N-N interaction Argonne v_{14} potential. The results have been obtained with a different method to compute the two-body G matrix, both for free nucleons and in nuclear matter, and solving the Brueckner equation directly in momentum space. The method mainly devised for the continuous choice of the single-particle potential has been tested both by calculating the two-nucleon phase shifts in some relevant channels and by performing a standard nuclear matter calculation within the gap choice. The results agree quite closely with previous calculations performed with separable forms of the N-N interactions, which are phase equivalent to the original potentials. This supports the use of these separable potentials in nuclear matter calculations since they appear sufficiently accurate. The calculations at the two-hole level of the nuclear matter saturation curve, obtained within the continuous choice, appear quite reliable and confirm that the scheme is able to incorporate most of the three-body correlations found within the gap choice. However, only a calculation of the three-hole-line contributions in the continuous choice[6] could substantiate this finding.

APPENDIX

In order to discretize Eq. (2), we split the integration interval in momentum space into a number of subintervals by means of a grid q_i,

$$I^{\alpha}_{LL'}(q,q',P;\omega)=\int q''^2 dq'' v^{\alpha}_{LL''}(q,q'')\frac{Q(q'';P)}{\omega-E(q'',P)} \times G^{\alpha}_{L''L'}(q'',q',P;\omega) = \sum_{i=1}^{N}\int_{q_i}^{q_{i+1}} dq \frac{F(q'',q',q,P;\omega)}{S(q'',P;\omega)} , \quad \text{(A1)}$$

TABLE III. Potential energy per particle in MeV for the Argonne v_{14} interaction in the continuous and gap choices for various values of k_F.

Channel	Gap $k_F=1.36$	Cont. $k_F=1.36$	Cont. $k_F=1.2$	Cont. $k_F=1.6$
$^1S_0$	−16.31	−16.51	−12.98	−21.75
$^3S_1$-$^3D_1$	−15.54	−19.09	−16.76	−20.63
$^3P_0$	−3.83	−3.83	−2.70	−5.62
$^3P_1$	11.06	10.56	6.66	19.18
$^1P_1$	4.13	3.94	2.55	6.97
$^1D_2$	−2.84	−2.82	1.63	−5.64
$^3D_2$	−4.16	−4.18	−2.51	−7.80
$^3P_2$-$^3F_2$	−7.60	−7.90	−4.70	−15.04
$^1F_3$	0.91	0.89	0.51	1.77
$^3F_3$	1.72	1.70	0.93	3.58
$^1G_4$	−0.48	−0.47	−0.24	−1.06
$^3G_4$	−0.77	−0.77	−0.39	−1.76
Kinetic energy	23.01	23.01	17.93	31.87
Total binding	−10.71	−15.47	−13.33	−15.93

where the function S is the energy denominator $\omega - E(q'',P)$ and the function F includes all the other quantities appearing in the numerator. In each subinterval, the function S is approximated by linear interpolation,

$$S(q'',P;\omega) \approx S_i + \frac{S_{i+1}-S_i}{q_{i+1}-q_i}(q''-q_i) , \tag{A2}$$

where $S_i = S(q_i,P;\omega)$. Taking a constant average value of the function F in each subinterval, namely, $\bar{F}_i = (F_{i+1}+F_i)/2$, each integral can be done analytically and one gets

$$I^{\alpha}_{LL'}(q,q',P;\omega) = \sum_{i=1}^{N} \frac{\bar{F}_i}{m_i} \ln \left| 1 + \frac{m_i}{S_i}(q_{i+1}-q_i) \right| , \tag{A3}$$

where

$$m_i = \frac{S_{i+1}-S_i}{q_{i+1}-q_i} . \tag{A4}$$

Rearranging the indices of the summation to single out the G matrix at the grid points, which needs to be calculated, one gets Eq. (4) shown in the text.

---

*Permanent address: Centro de Física, da Matèria Condensada Avenida Gama Pinto 2, 1699 Lisboa, Portugal.

[1]B. D. Day, Rev. Mod. Phys. **50**, 495 (1978), and references therein.
[2]R. Rajaraman and H. Bethe, Rev. Mod. Phys. **39**, 745 (1967).
[3]B. D. Day, Phys. Rev. C **24**, 1203 (1981).
[4]B. D. Day and R. B. Wiringa, Phys. Rev. C **32**, 1057 (1985).
[5]J. P. Jeukenne, A. Legeunne, and C. Mahaux, Phys. Rep. C **25**, 83 (1976).
[6]M. Baldo, I. Bombaci, G. Giansiracusa, U. Lombardo, C. Mahaux, and R. Sartor, Phys. Rev. **41**, 1748 (1990); M. Baldo, I. Bombaci, G. Giansiracusa, and U. Lombardo, J. Phys. G **16**, L263 (1990).
[7]J. Heidenbauer and W. Plessas, Phys. Rev. C **30**, 1822 (1984); **32**, 1424 (1985).
[8]M. Baldo and L. S. Ferreira, Phys. Lett. B **255**, 477 (1991).
[9]J. P. Lejeune, P. Grangé, M. Martzolff, and J. Cugnon, Nucl. Phys. **A453**, 189 (1986).
[10]M. A. Matin and M. Dey, Phys. Rev. C **27**, 2356 (1983).
[11]C. Mahaux and R. Sartor, in *Nuclear Matter and Heavy-Ion Collisions*, edited by H. Flocard and M. Soyeur (Plenum, New York, 1990).
[12]M. Baldo, Nucl. Phys. **A519**, 243c (1990).
[13]M. Baldo and L. S. Ferreira, Phys. Rev. C **41**, 2298 (1990).
[14]R. B. Wiringa, R. A. Smith, and T. L. Ainsworth, Phys. Rev. C **29**, 1207 (1984).